SUPPORTING MATERIAL

1. SUPPLEMENTARY FIGURES

Figure S1. Density profiles of the 4 shallow cores. Density data for the 2012 core are from Spolaor et al. (2013) while density data for the 2015 core are from Ruppel et al. (2017). Density of the 2017 and 2019 cores are from this work.

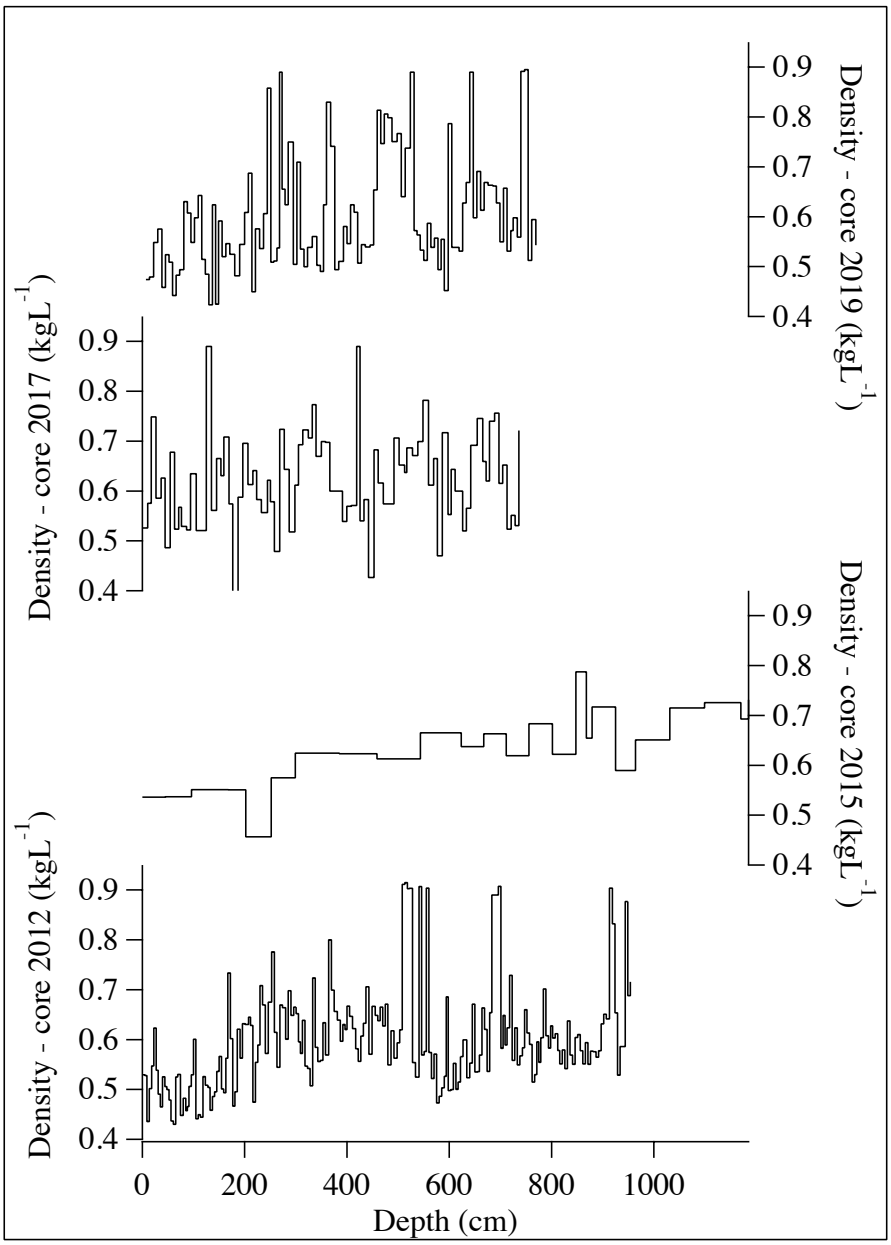

Figure S2. Estimated precipitation (in mm w.e.) at the summit of the Holtedahlfonna site during the period 1991-2020. The lower panel shows the amount of seasonal precipitation and the estimated total precipitation (sum of the four seasons), the middle panel shows the relative contribution of the seasonal precipitation (0 min–1 max) for each year, while the upper panel shows the trend of seasonal precipitation.

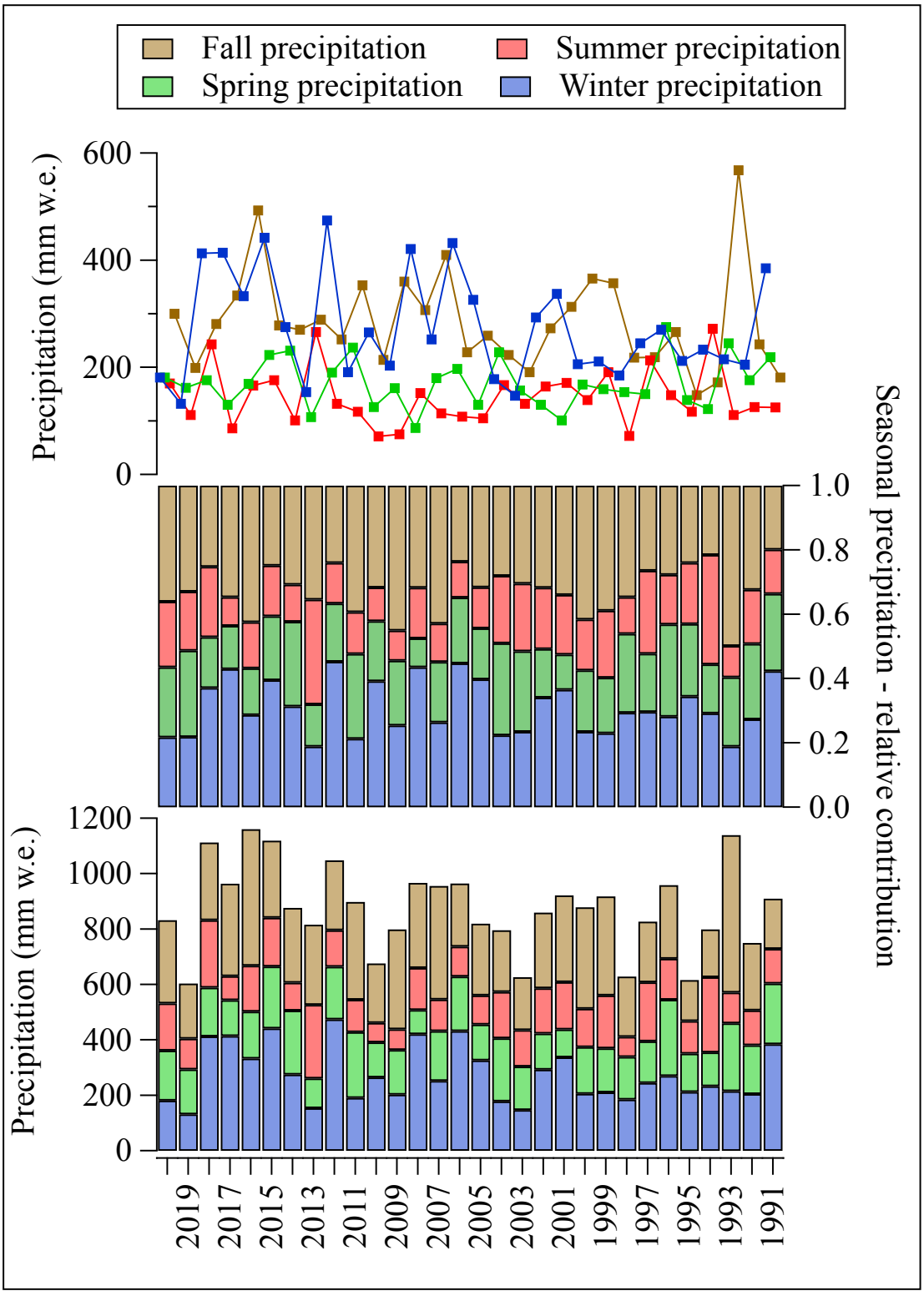

Figure S3. Model estimate of the seasonal Positive Degree Days (PDD) and the seasonal melt at the top of the Holtedahlfonna site. Note that both y-axes are split. There are high PDD and melt values during summers (JJA) but both can occur also in fall (SON) and spring (MAM - 2002 and 2011)

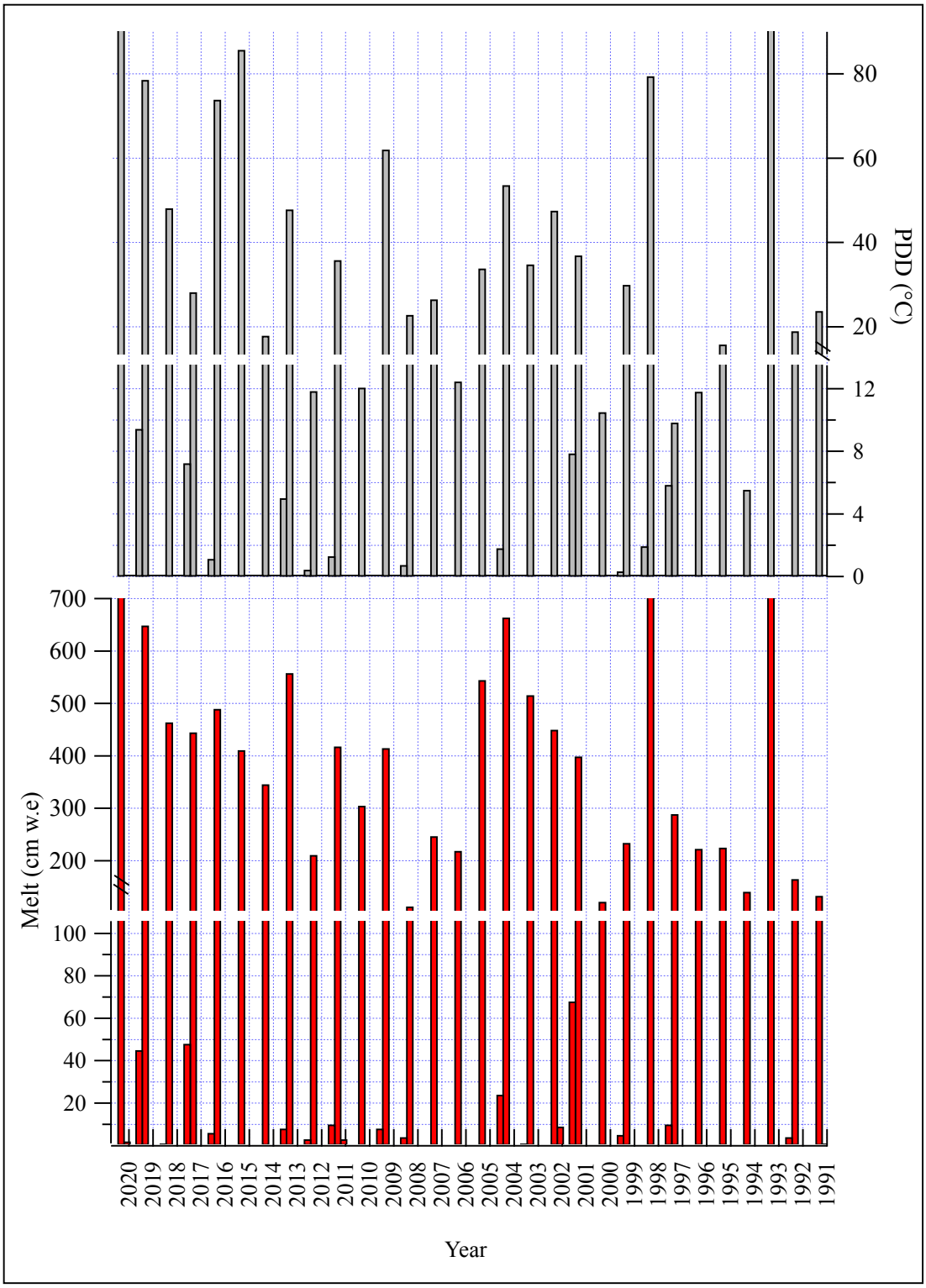

Figure S4. Monthly temperature estimates at the summit of the Holtedahlfonna ice field from the HARMONIE-AROME model for the period 2004-2020

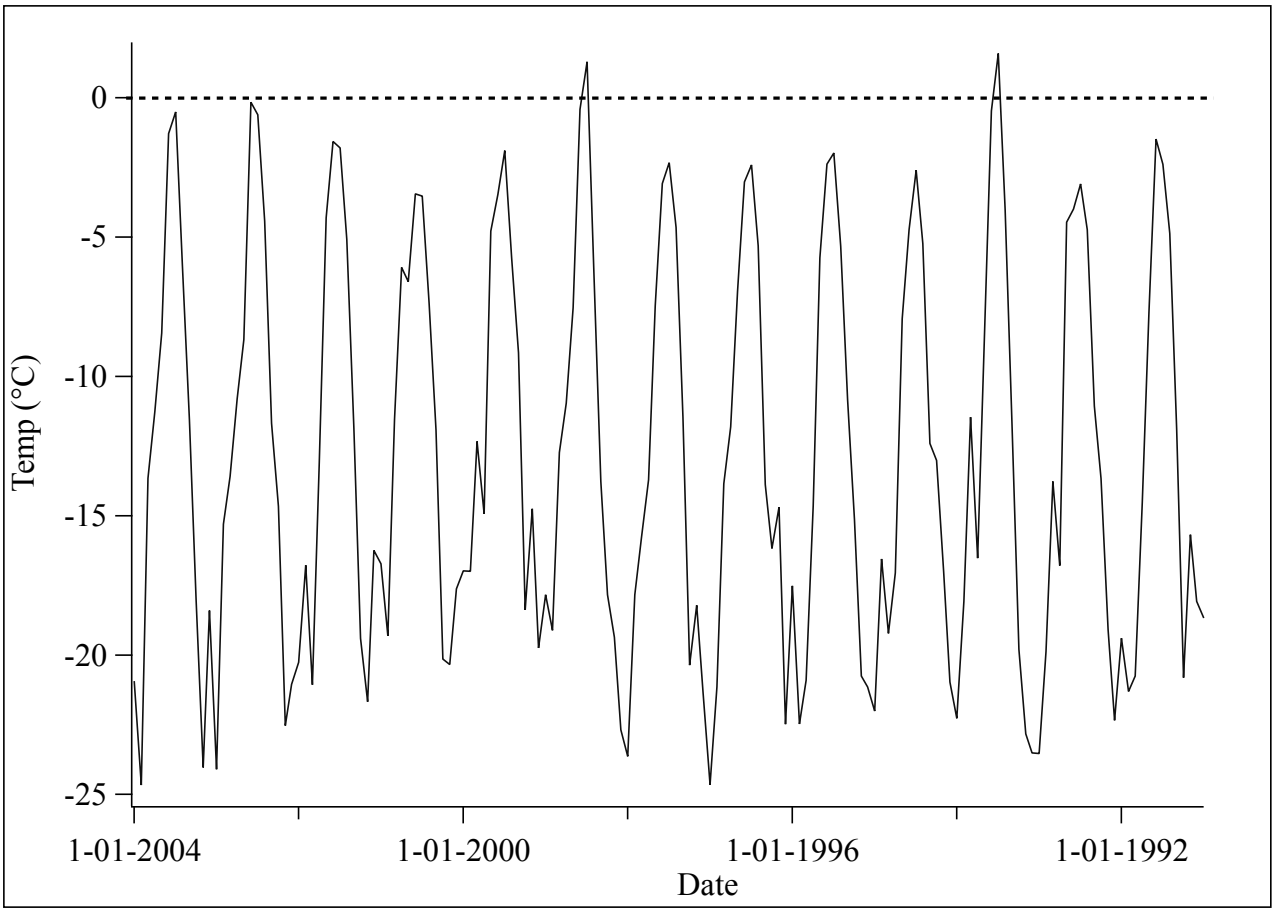

Figure S5. Seasonal cycle of the $\delta^{18}O$ in the core drilled in 2005 at the same site (Divine et al 2011). for the period 1960-2000. Green and white colors identify each year.

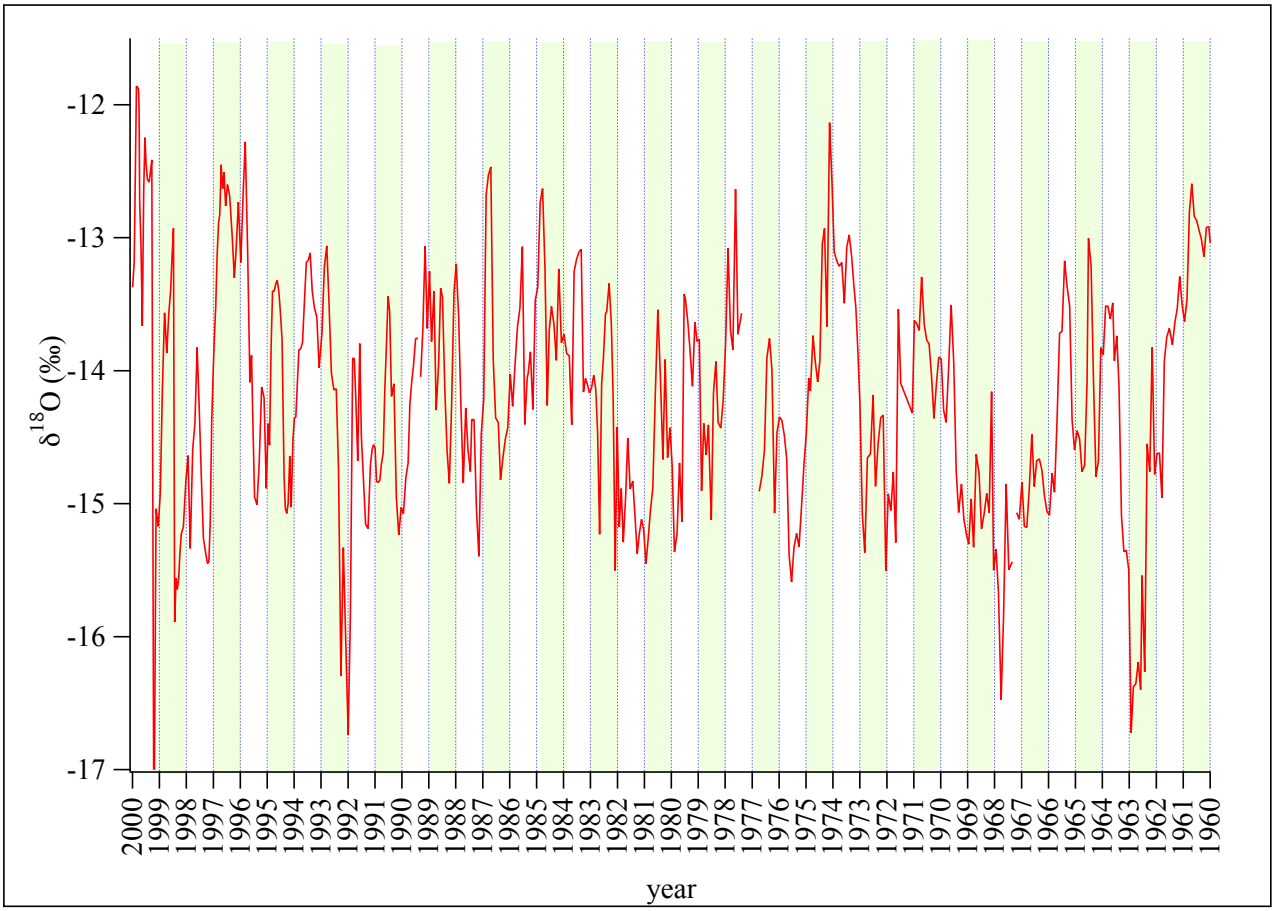

2. STATISTICAL ANALYSIS

2.1 Linear regression model

To determine the annual oscillation of the $\delta^{18}O$ signal in the four shallow cores statistically, we used a linear regression model to test the seasonality of the $\delta^{18}O$ isotopic signal on each ice coreas determined from the measured mass balance. For each core and each year, we first identified the maximum and the minimum for the $\delta^{18}O$ signal (Figure S6) and then calculated the weighted slope between each extreme value (Figure S7) using the formula:

$$S_i = \frac{\delta 18O_{i+1} - \delta 18O_i}{l_{i+1} - l_i} W_i$$

where $d^{18}O_i$ is the annual extreme (maximum or minimum), l_i is the layer depth that corresponds to the $d18_i$ and W is the weight calculated as:

$$W_i = [\delta 18O_{i+1} - \delta 18O_i] \,/\, \sum_{i=1}^{n} [\delta 18O_i]$$

To test for the statistical significance of the seasonality, we applied a regression equation that tests the conditional mean of the weighted slope based on the increase and decrease of the slope. The equation to be tested is:

$$S_i = \sum_{i=1}^{2} \beta_i \, K_i$$

Where $K_1 = 1$ for decreasing slope and 0 for increasing slope, $K_2 = 1$ for increasing slope and 0 for decreasing slope and β_i is the coefficient of the model to be tested. The significant values of the seasonality of the weighted slope considering the increasing and decreasing periods separately is presented in Table S1. A significant seasonality (p-value < 0.05) is only observed in 2012 and 2015 ice cores.

Table S1. Significant values of the coefficients of the regression model based on the magnitude of the slope (positive or negative).

Ice core	*p - value* for decreasing slope (-)	*p - value* for increasing slope (+)
2012	**0.048**	**0.027**
2015	**0.004**	**0.007**
2017	0.082	0.497
2019	0.121	0.260

Figure S6. Identification of the annual minimum and maximum values of $\delta^{18}O$ (red and blue points) based on the annual mass balance dating for the four shallow cores.

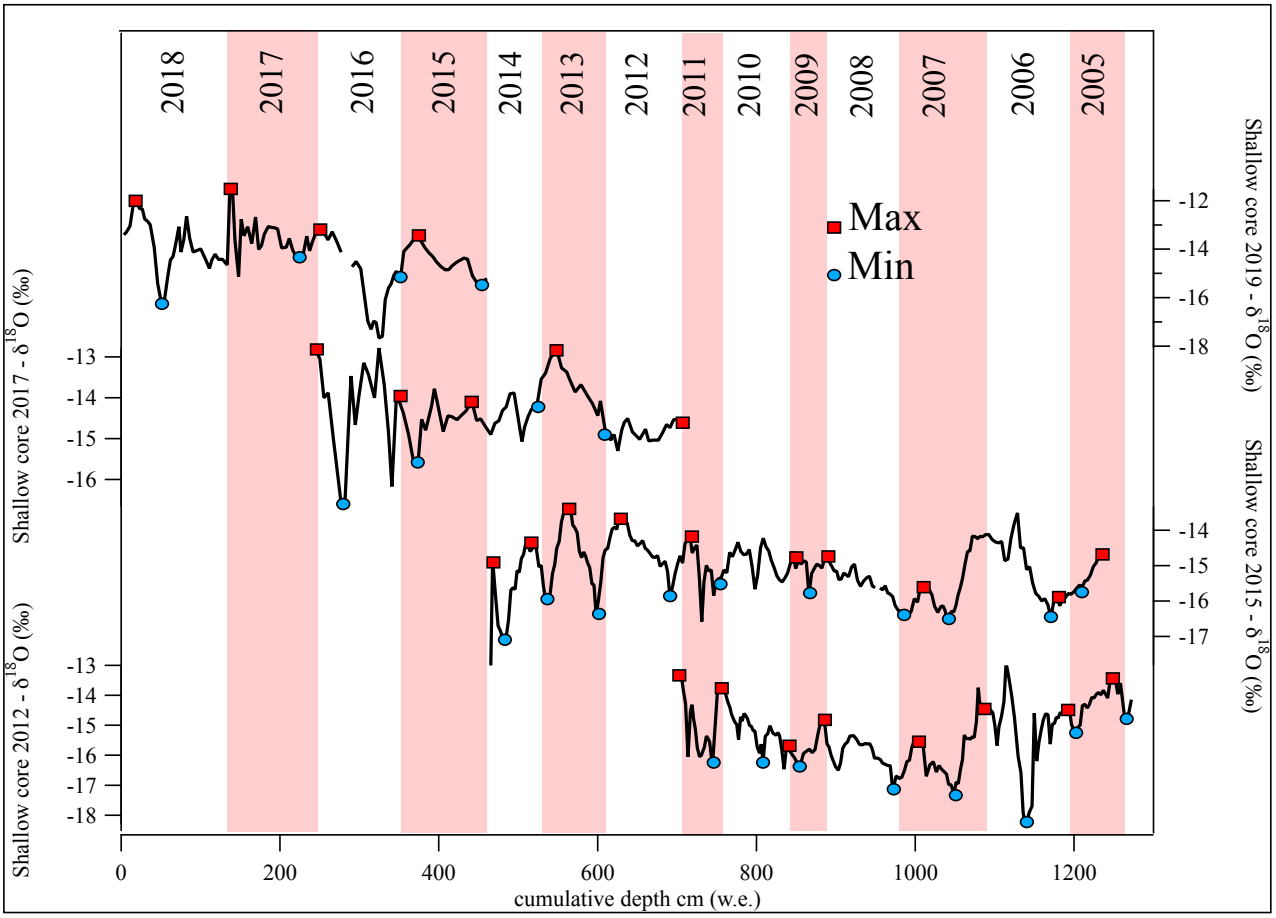

2.2 Spectral analysis

Spectral analysis of the core's points to deterioration of the climatic signal archived in the isotopic composition. Since the power spectral density does not include the phase of the signal, it is possible to compare the four cores regardless of the period they cover. We compute the power spectral density only on the upper three meters of each core, both to study the signal initially preserved, and to limit the impact of isotopic diffusion, which increases with depth and is visible at high frequency (decrease of the PSD above 2.10-2 cm^{-1}). At low frequency (below the seasonal cycle depth length equivalent), we observe the noise added by the aliasing of the seasonal cycle though stratigraphic noise (Laepple et al, 2018). We compare the four cores with a virtual core generated by computing the impact of precipitation intermittency on the isotopic signal, following Casado et al, (2020). This virtual firn core represents the most accurate archived signal for the site. The firn core of 2012 almost matches this ideal situation, where the interannual noise level matches one of the simulations (around 4 ‰ cm), and with the amplitude of the seasonal cycle roughly 3.5 times larger than the noise level (seasonal signal to noise ratio, or SNR of 3.5 for the 2012 core). The noise level increased in the 2015 core, leading to a SNR of only 1.5. For the 2017 and 2019 cores, the noise level is larger than the amplitude of the seasonal cycle, equivalent to SNR below 1. Since the virtual core considers precipitation intermittency, this indicates that processes occurring at the surface of the firn (namely sublimation and condensation, wind redistribution, and percolation) have had an increasing contribution to the water isotope signal at this site. This is observed by a decrease in the SNR, which limits the interpretation at time scales ranging from annual to decadal for this site.

Figure S7. Spectral analysis of the four firn cores. The cores were compared with a virtual core (gray) generated by computing the impact of precipitation intermittency on the isotopic signal.

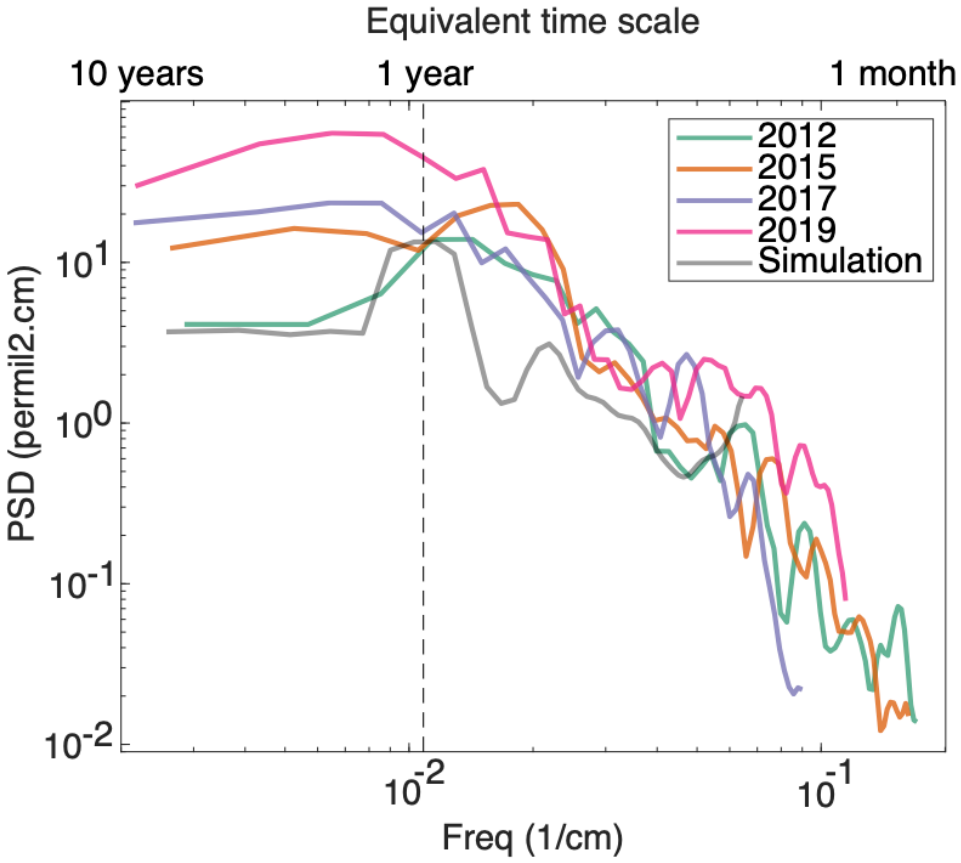

REFERENCES

Casado, M., Münch, T. & Laepple, T. Climatic information archived in ice cores: impact of intermittency and diffusion on the recorded isotopic signal in Antarctica. Clim. Past 16, 1581–1598 (2020).

Divine, D., Isaksson, E., Martma, T., Meijer, H. A. J., Moore, J., Pohjola, V., van de Wal, R. S. W., & Godtliebsen, F. (2011). Thousand years of winter surface air temperature variations in Svalbard and northern Norway reconstructed from ice-core data. *Polar Research*, *30*(1), 7379. https://doi.org/10.3402/polar.v30i0.7379

Laepple, T. et al. On the similarity and apparent cycles of isotopic variations in East Antarctic snow pits. Cryosph. 12, 169–187 (2018).

Ruppel, M. M., Soares, J., Gallet, J.-C., Isaksson, E., Martma, T., Svensson, J., Kohler, J., Pedersen, C. A., Manninen, S., Korhola, A., & Ström, J. (2017). Do contemporary (1980–2015) emissions determine the elemental carbon deposition trend at Holtedahlfonna glacier, Svalbard? Atmospheric Chemistry and Physics, 17(20), 12779–12795. https://doi.org/10.5194/acp-17-12779-2017

Spolaor, A., Gabrieli, J., Martma, T., Kohler, J., Björkman, M. B., Isaksson, E., Varin, C., Vallelonga, P., Plane, J. M. C., & Barbante, C. (2013a). Sea ice dynamics influence halogen deposition to Svalbard. The Cryosphere, 7(5), 1645–1658. https://doi.org/10.5194/tc-7-1645-2013